Supporting Information

Receptor displacement in the cell membrane by hydrodynamic force amplification through nanoparticles

Silvan Türkcan,[1] Maximilian U. Richly,[1] Cedric I. Bouzigues,[1] Jean-Marc Allain[2] and Antigoni Alexandrou[*,1]

[1]Laboratoire d'Optique et Biosciences, CNRS, INSERM U696, 91128, Palaiseau, France

[2]Laboratoire de Mécanique des Solides, CNRS, 91128, Palaiseau, France

*Corresponding author: Antigoni Alexandrou

Email : antigoni.alexandrou@polytechnique.edu, jean-marc.allain@polytechnique.edu

Tel : +33 1 69 33 50 04

Movie S1: Displacement of a CPεT receptor on an MDCK cell surface during application of a low flow rate of 10 µL/min (0.0032 m/s) due to the drag force F_d. In the beginning, no flow is applied and the receptor undergoes Brownian motion in a confining domain. When indicated, the flow is turned on and the receptor is displaced upwards in the flow direction. When the flow is turned off at t=5.3 s, the receptor returns close to its initial position. At t=7.2 s, we switched to white light illumination to verify that the cell contours did not move.

Movie S2: Displacement of a CPεT receptor on an MDCK cell surface during application of a high flow rate of 30 µL/min (0.0096 m/s) due to the drag force F_d. In the beginning, no flow is applied and the receptor undergoes Brownian motion in a confining domain. When indicated, the flow is turned on and the receptor is displaced upwards in the flow direction. The larger drag force F_d forces the CPεT receptor to cross the first barrier it encounters (see jump at t~5.1 s) and forces it against a second barrier. After the flow is turned off at t=11.6 s, the receptor relaxes back close to the position of the undeformed second barrier and does not return to its initial position before the flow cycle.

NP-toxin conjugate adsorbed to the glass surface

Figure S1 shows the positions of a NP-toxin conjugate adsorbed to the glass surface. The maximum flow (30 µL/min) that is typically used in the experiments is applied. Compared to trajectories of NPs bound to toxin receptors on cells, the apparent "displacement" along the flow direction is about orders of magnitude smaller and is dominated by the positioning noise due to the limited number of collected photons.

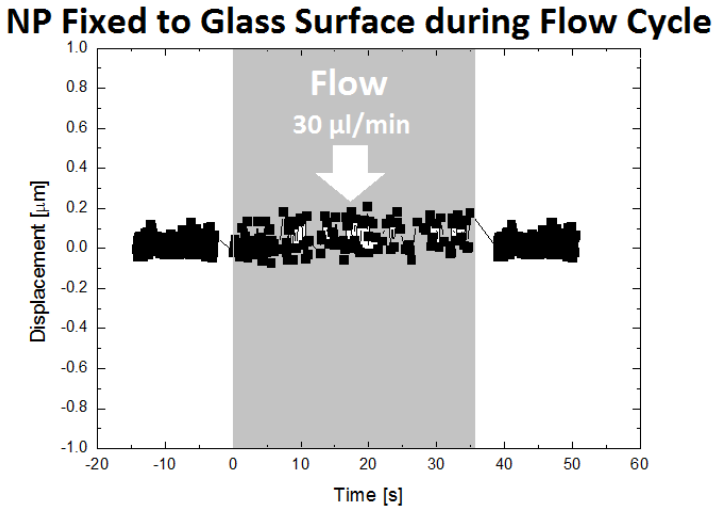

Fig. S1: Nanoparticle position in the direction along the flow as a function of time during application of the maximum flow used in the experiments. The apparent "displacement" with and without flow is almost identical. The rms value of the motion perpendicular to the flow direction is 0.056 µm. We use a brief flash of white light to indicate the beginning and end of flow application resulting in a series of non-analyzable frames.

Determination of the flow speed around the nanoparticles

We determine the flow speed of the liquid around the nanoparticle by particle velocimetry (PIV), using unbound nanoparticles in solution. We grow cells in the microchannels, let toxin-conjugated nanoparticles bind to their specific receptors in the cell membrane, and focus the microscope objective at the nanoparticle positions in the same conditions as in the experiments. We then add a flow of nanoparticles and measure the displacement of unbound nanoparticles which are in focus, i.e. located in the same focal plane as the membrane-bound nanoparticles. Nanoparticle trajectories showing a slowing down due to transient interactions with the membrane were not analyzed. Figure S2 shows the measured flow speed from unbound nanoparticles (black squares) for different flow rates up to 0.6 µL/min. For higher flow rates, we do not have enough signal to track the faster fraction of the passing nanoparticles which yields an underestimation of the velocity. We therefore use a linear fit of the four PIV measurements shown in Fig. S2 and extrapolate this fit to determine the flow velocity corresponding to higher flow rates.

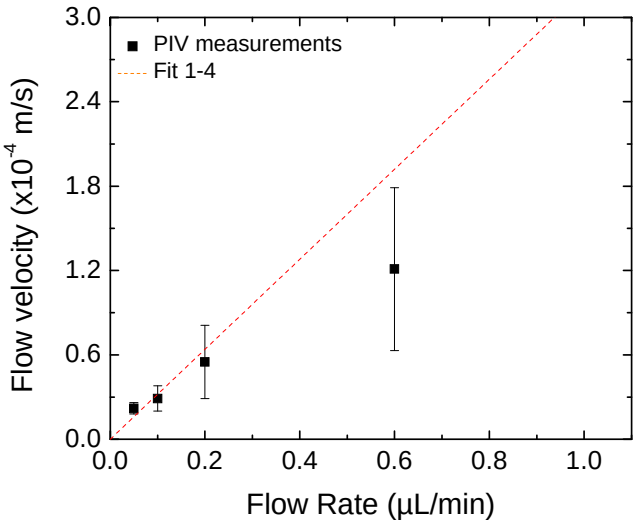

Fig. S2: Measured flow speed as a function of flow rate (black squares) determined from unbound nanoparticles flowing above the cell at the same height as that of receptor-bound toxin-conjugated nanoparticles. The measured flow velocity shown is the average of 10, 10, 53, and 8 different nanoparticles for the flow rates of 0.05, 0.1, 0.2, and 0.6 µL/min, respectively. The error bars indicate the standard deviation of these measurements. The linear fit of these PIV measurements is given by the dashed red line that has a slope of $3.2 \pm 0.8 \times 10^{-4} \; \frac{\frac{m}{s}}{\frac{\mu L}{\min}}$.

The accuracy of our speed measurement of nanoparticles flowing in the cell surface focal plane is limited by the depth of field (DOF) of our microscope objective (500 nm), due to the fact that, because of the proximity of the cell surface, we are essentially measuring the speed of nanoparticles located in the range [z,z+DOF/2]. Using the Poiseuille equation with the slip length determined above, we estimate that this effect may lead to an overestimation of the flow velocity of 20% which is within the error bar of the velocity determination.

We thus measured flow velocities that are much higher than expected from the Poiseuille equation assuming a no-slip boundary at the water-cell interface. Indeed, cells are not hard boundaries and a non-zero slip length is associated to them. We can, however, use the Poiseuille equation assuming that the vertical position z indicates the distance from the virtual zero-flow plane:

$$v(z) = v_{mean}(-\frac{4}{h^2})(z^2 - hz),$$

$$v_{mean} = \frac{3U}{2A}$$

where h is the total height of the channel (30 μm), A the cross section of the channel (12000 μm²), and U the flow rate. Our PIV measurements can be reproduced with a value of z= 800±200 nm. Since the distance of the nanoparticle from the cell surface is negligible compared to this distance value, this distance value corresponds to the slip length of our system.

The drag force on the particle can be estimated using:

$$\vec{F}_d = 6\pi\eta_{eff} r\vec{v}_{flow}.$$

where r the hydrodynamic radius of the nanoparticle and v_{flow} the flow velocity and η_{eff} the effective viscosity of the liquid. When the nanoparticle is located on the order of one nanoparticle radius or less away from the zero-flow plane, hydrodynamic flow modifications around the nanoparticle modify this drag force. This effect can be described by introducing an effective viscosity, η_{eff} different from the bulk liquid viscosity η. However, because of the large slip length in our case, the particle is more than 25 times the nanoparticle radius away from the v=0 μm/s boundary. As a consequence, the distortion of the fluid flow around the nanoparticle is negligible and η_{eff} can be taken to be equal to the water viscosity η_{water}=0.001 Pa.s.

The mean radius of the nanoparticle was determined to be 28 nm (with a standard deviation of 8 nm) using the number of collected photons, as discussed in Ref. [1]. The error on this determination was shown to be 10% [1]. The radius of each individual NP was used for the force determination. The exerted drag force F_d thus ranges from 0.42±0.05 pN to 8±18 pN for flow rates of 2.5 to 50 μL/min, as shown in the following table for a NP with a radius of 28 nm. The error on the force determination was determined from the error on the velocity and on the nanoparticle radius and is dominated by the second one.

Flow Rate [µL/min]	Fd [pN]	Error on Fd [pN]	% Error
2.5	0.42	0.05	12
5	0.83	0.2	24
7.5	1.2	0.4	33
10	1.7	0.7	41
15	2.5	1.6	64
20	3	3	100
30	5	7	140
50	8	18	225

Table: F_d calibration with estimated error.

Additional receptor trajectories during flow cycles

Figure S3 shows additional CPεT toxin receptor trajectories during a flow cycle.

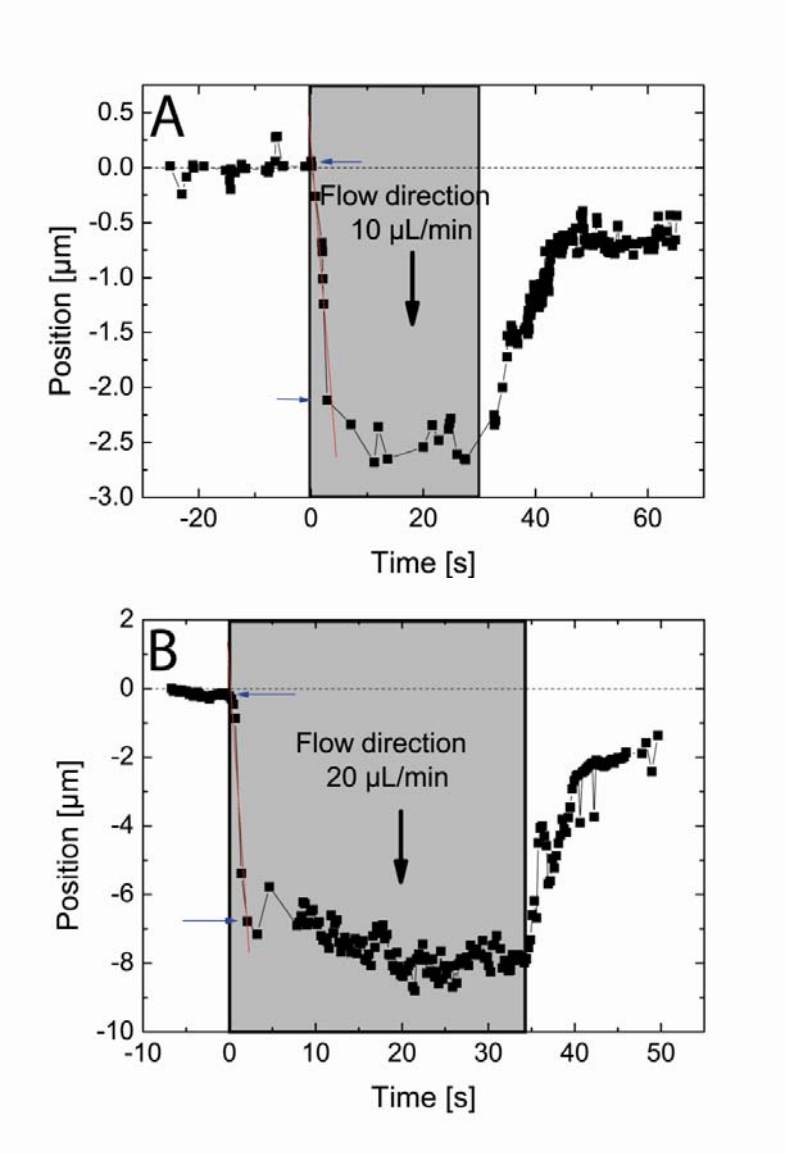

Fig. S3: Trajectories of a CPεT receptor marked by a NP. The flow of medium produces a drag force F_d while the flow is on (grey zone). The flow is started at t=0 s. The red line is a linear fit to the displacement of the receptor versus time after the flow is turned on between the time points marked by blue arrows.

Cell stability during flow

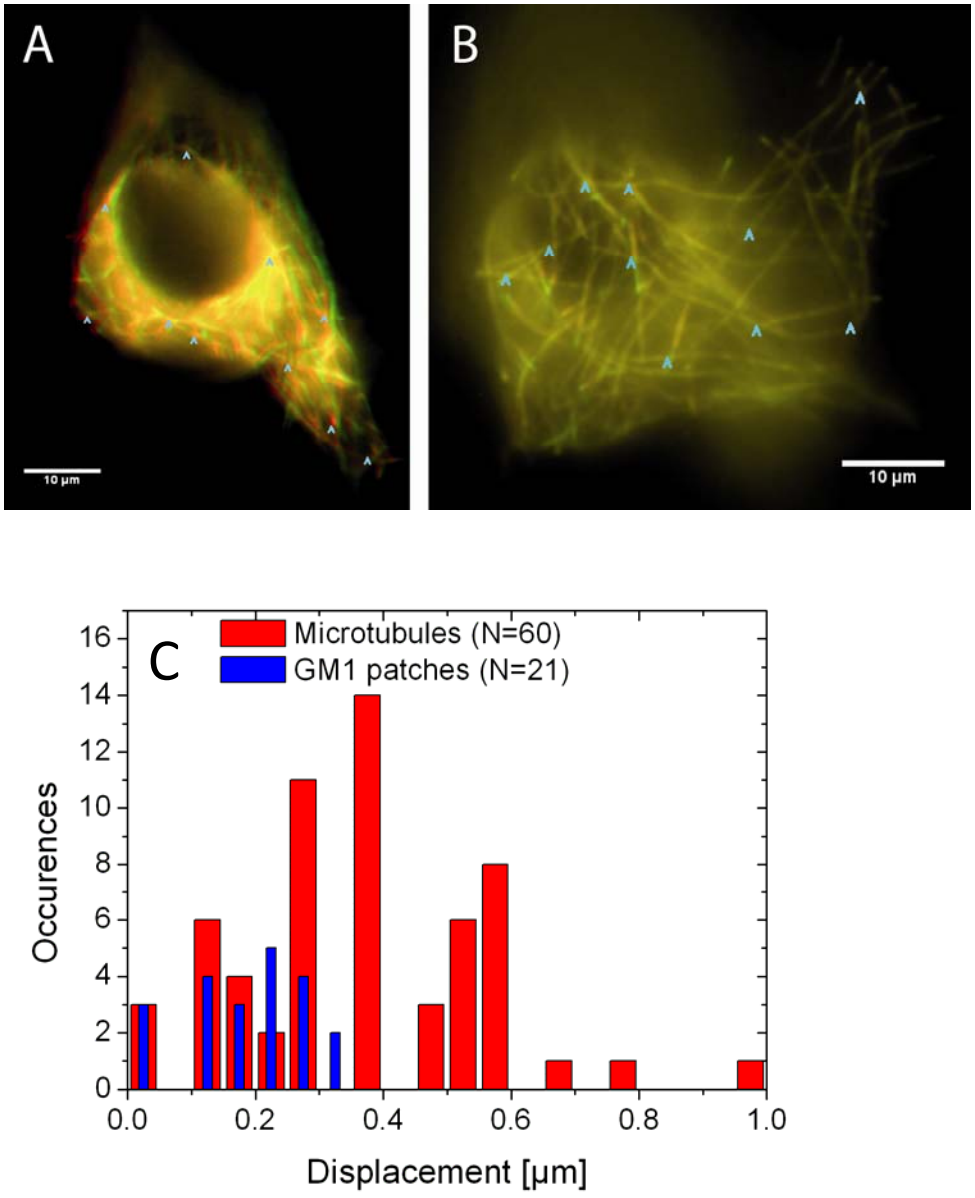

Fig. S4: (A & B) EB3-GFP labeled microtubules of two cells without fluid flow in red and under a flow rate of 50µL/min (flow velocity: 0.01 m/s) in green. This flow rate is the maximal flow rate used during single-molecule experiments. Arrows indicate points of measurements of the displacement. (C) Histogram of displacement measures from microtubules (red) and GM1 patches (blue).

Imaging of cells labeled with GFP-actin during flow cycles

Figure S5 shows cells transfected with a reduced expression GFP-β actin plasmid (Addgene plasmid 31502) [2] after 25 hours of incubation.

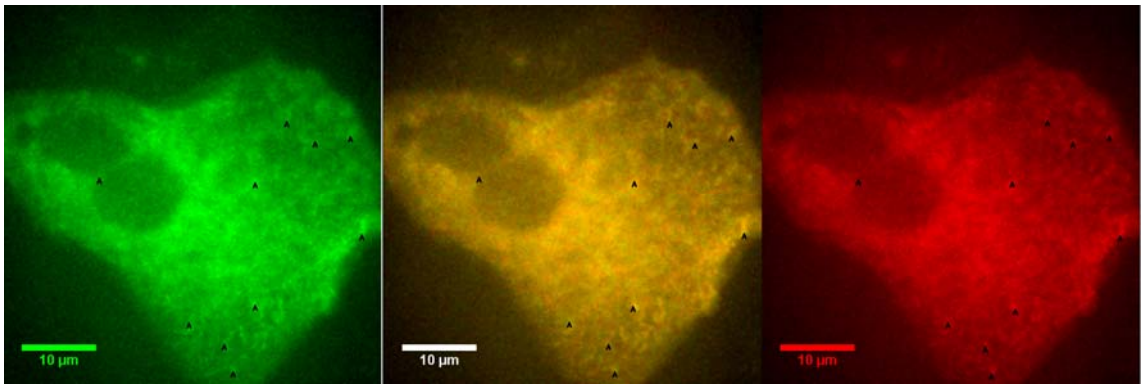

Fig. S5: A superposition of two images (yellow) of the same cell labeled with GFP-actin before (green) and during (red) application of the maximum flow (30 µL/min). The average displacement of the actin segments indicated with black arrowheads is 0.36±0.06 µm (N=10).

Actin labeling with phalloidin-rhodamin before and after flow cycles

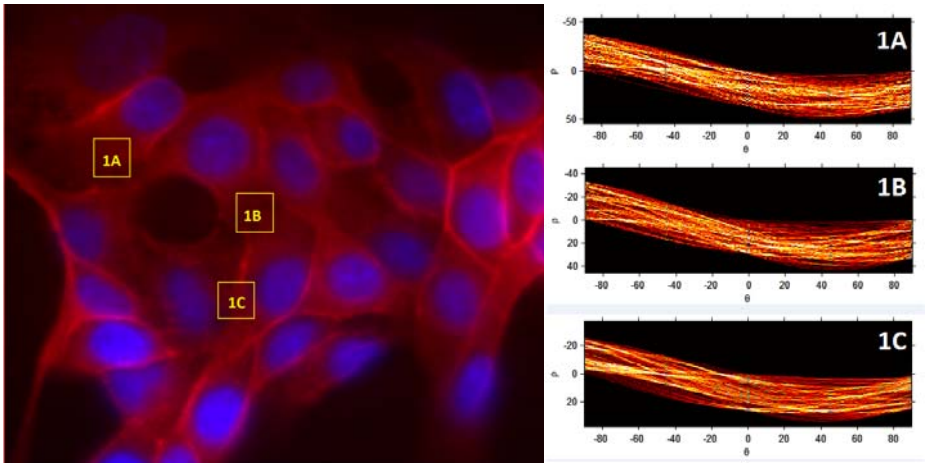

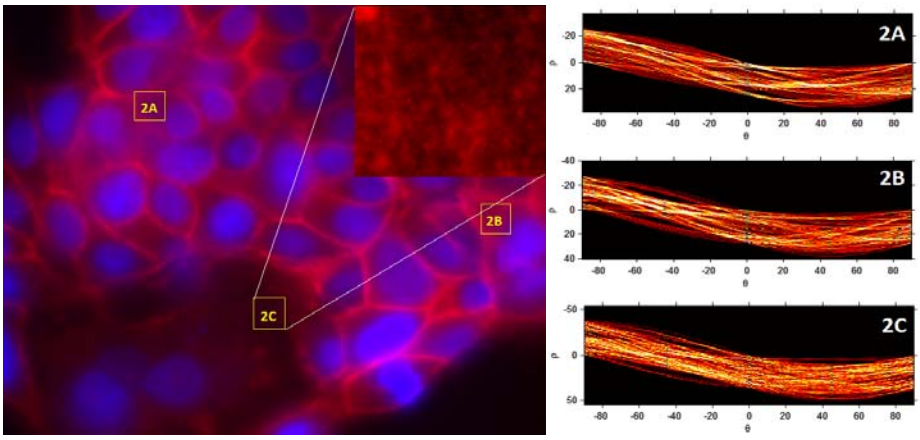

Fig. S6: Two sets of MDCK cells fixed before (above) and right after a flow cycle (below) for focusing at the apical cell membrane. Actin is labeled with phalloidin-rhodamin (red) and the nuclei are labeled with DAPI. The Hough transforms are shown for selected subareas of the image indicated with rectangles. The homogeneous intensity distribution of the Hough transform images indicates that there is no preferential orientation of the actin filament neither before nor after a flow cycle. Total image width is 81.9 µm.

Raft labeling with sphingomyelin-BODIPY during flow cycles

Figure S7 shows the apical side of MDCK cells incubated with sphingomyelin-BODIPY which labels lipid rafts within the cell membrane. They is no significant raft movement even under maximum flow conditions (30 µL/min).

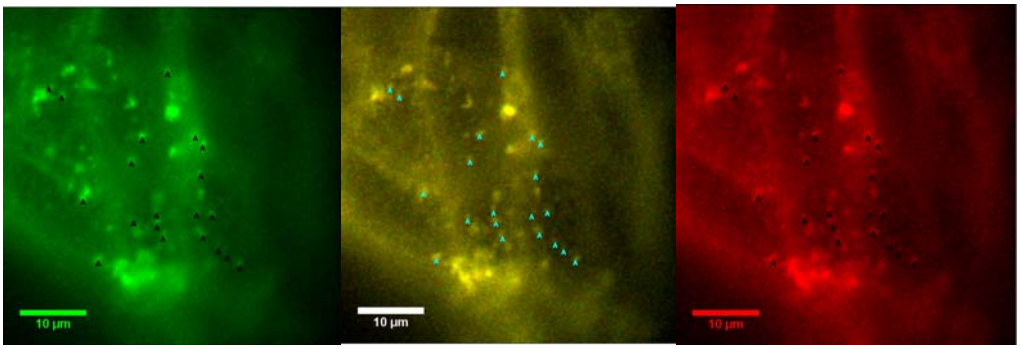

Fig. S7: A superposition (yellow) of sphingomyelin-BODIPY labeled cellular membrane before (green) and during (red) maximum flow (30 µL/min). The change in position of the rafts indicated with light blue and black arrowheads) was measured to be on average 0.34±0.03 µm (N=20 on 6 cells).

Inferred confinement potential during a flow cycle

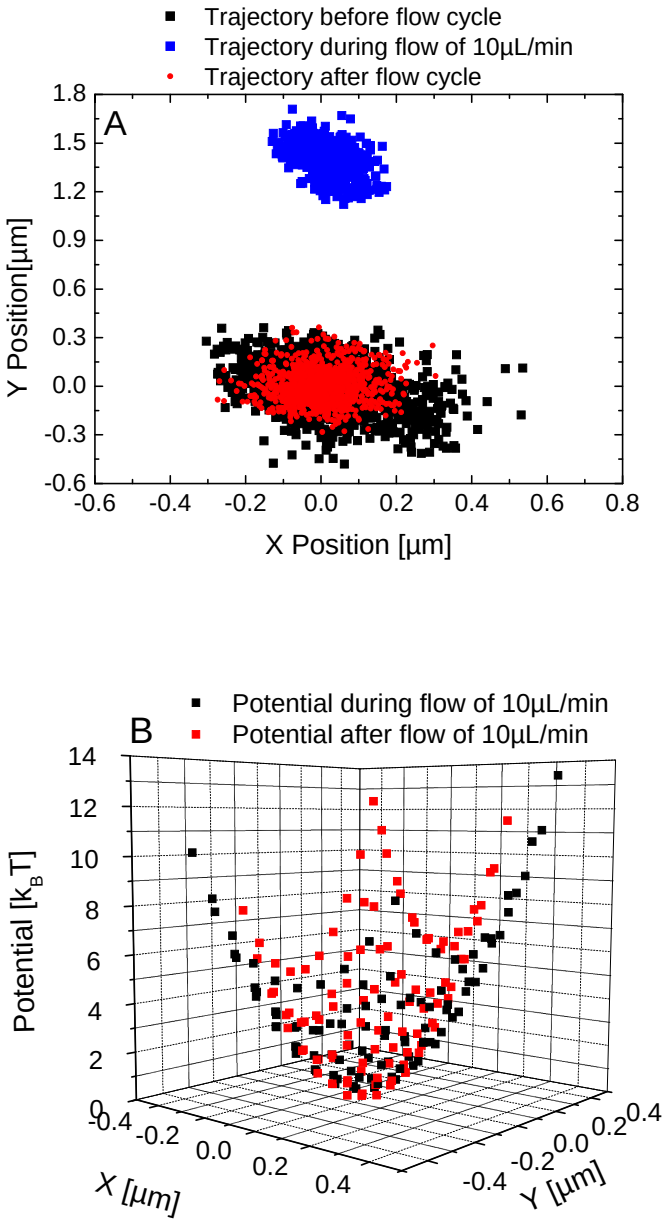

Fig. S8: Trajectory (A) and inferred potential (B) of a single CPεT receptor during a flow cycle. The inferred diffusion coefficient before (black trajectory in A) and after flow (red trajectory in A) is 0.068 ± 0.002 and 0.051 ± 0.002 µm²/s, respectively. The domain radius (defined as the radius of a circle including 95% of the trajectory points) is 0.35±0.03 µm before and 0.24±0.03 µm after the flow. The confining potential has been shown to be spring-like and the determined spring constant before and after flow is 0.44 ± 0.03 pN/µm and 0.91 ± 0.06 pN/µm, respectively.

Receptor trajectories during flow cycles before and after incubation with COase

Figure S9 shows the trajectory of a CPεT receptor during a flow cycle before and after incubation with cholesterol oxidase. Note that, after incubation with cholesterol oxidase, the amplitude of the receptor movement before, during flow (after an equilibrium position is reached), and after the flow is stopped is larger because the confinement domain size is larger. The general behavior, however, is similar: the receptor is displaced during the flow and returns back close to its initial position after the flow is stopped.

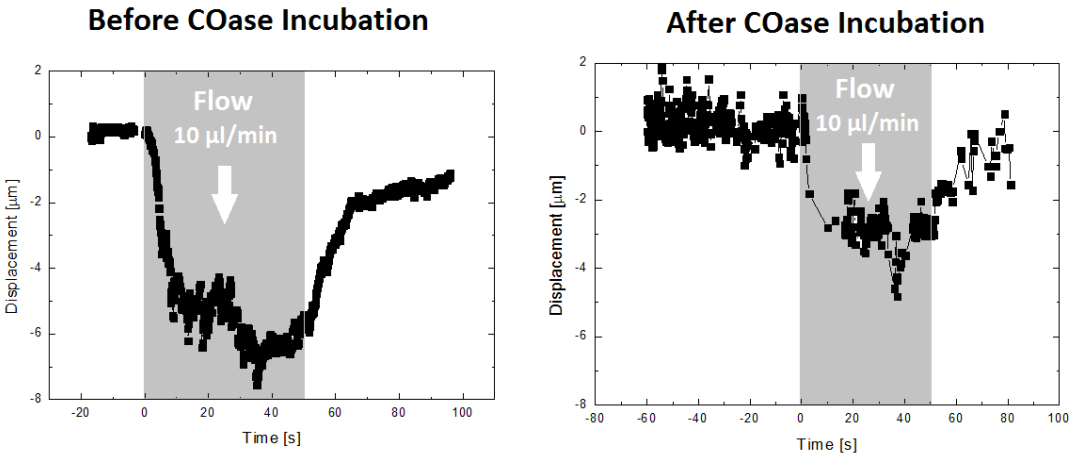

Fig. S9: Toxin receptor displacement along the flow direction as a function of time upon application of a flow of 10 µL/min without (left) and with (right) incubation with 20 U/µL of cholesterol oxidase. The grey rectangles indicate the time periods when the flow is on.

Model of receptor movement under force

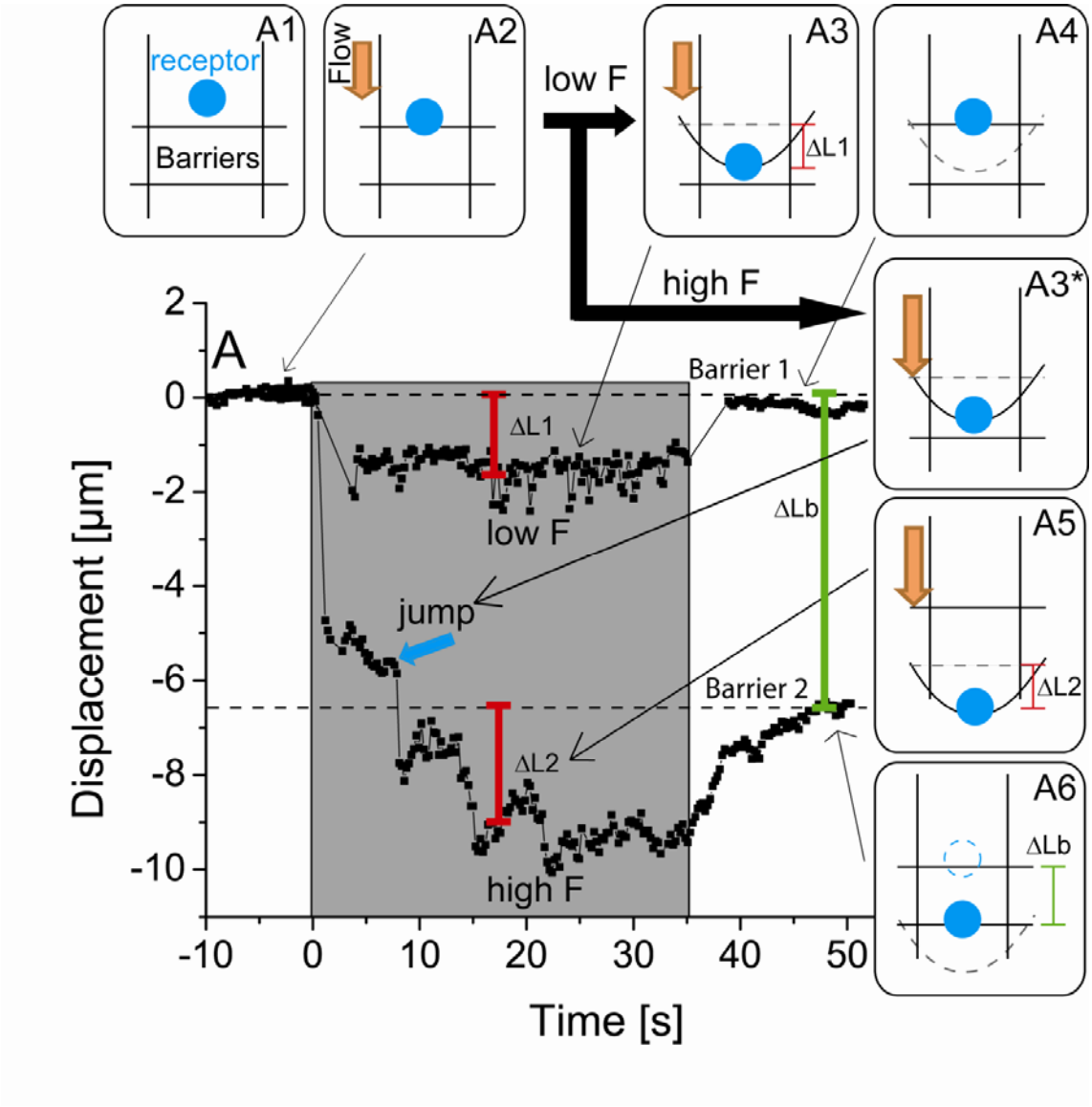

Fig. S10: Model of receptor movement under external force. The blue dots represent the receptor and NP position and the black lines represent cytoskeleton barriers. (A) Displacement of a receptors due to an applied force, starting at t=0 s. The flow is present during the time indicated by the grey region. When the flow starts, the receptor labeled with a NP is displaced until it encounters a barrier (A1 & A2). This may happen the first time an external force is applied. The force on the receptor will then deform the barrier until the drag force F_d balances out the restoring force of the flexible barrier (A3). At this point, barrier 1 (dashed black line) is deformed (solid black line) by ΔL1 (red), which we measure by averaging the points before the flow was started and subtracting the average position during flow, when the equilibrium position has been reached. When the flow is stopped (A4), the barrier returns close to its initial position (solid black line) pulling the receptor back with it. However, in other cases, the drag force F_d is large enough (high F) to force the receptor over a barrier (A3* to A5 & blue arrow in A). The receptor then encounters and is forced against a

second barrier (A5) (barrier 2 dashed line) and deforms it by a distance ΔL2 (red). When the flow is turned off, the receptor will not return to its initial position (y=0 µm), but only to the position to which it is restored by the second barrier (A6). Having observed both barriers, their distance ΔLb (green) can be measured by calculating the difference between the mean position to which the receptor relaxed initially and the mean position to which the receptor relaxed after jumping over the barrier.

Spring constant of the barriers after treatment with latrunculin B

The spring constant of the barriers is determined by fitting the displacement of the receptor due to flow with Hooke's law. After incubating the cells for 30 minutes with 500 nM latrunculin B, we recorded displacement versus flow curves, as shown in Fig. S11.

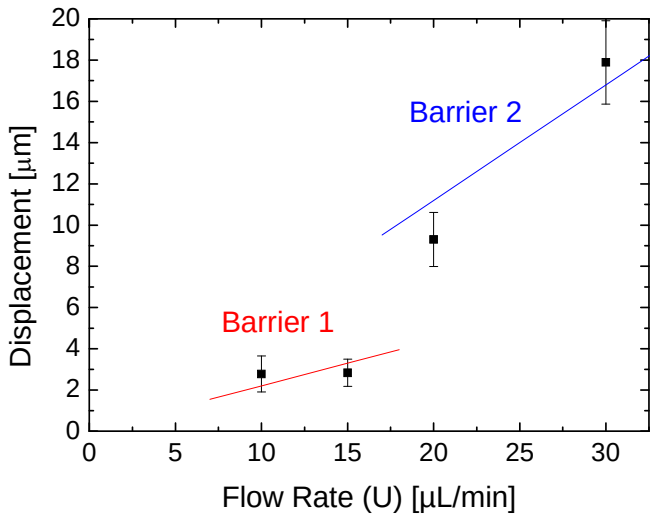

Fig. S11: Displacement of a CPεT receptor due to the drag force F_d that is created by a fluid flow after incubation with latrunculin B. The displacement values are obtained by averaging all the recorded positions during flow (after the equilibrium position is reached) and subtracting the mean position of the receptor before the flow was started. This particular receptor encounters two distinct barriers. From the linear fits (red and blue line), we can calculate the spring constants associated to the two barriers to be 0.70 ± 0.09 pN/µm for barrier 1 and 0.28 ± 0.01 pN/µm for barrier 2.

Additional trajectories fitted with the Kelvin-Voigt model

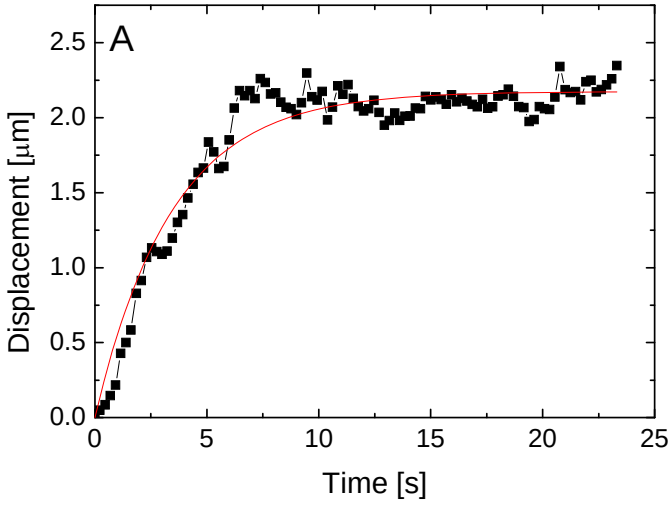

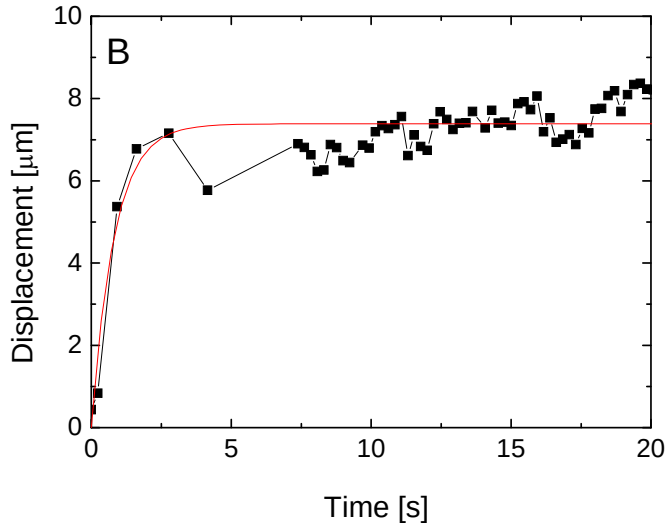

Fig. S12: Displacement of CPεT receptors due to a flow rate of 2.5 µL/min (A) and 20 µL/min (B) (flow velocity: 0.0008 m/s and 0.0064 m/s, respectively), which starts at time t=0 s. Note that we here show the absolute value of the displacement, in contrast to the displacement curves shown in Figs. 1, 3, and 4. The drag force displaces the receptor until it reaches an equilibrium position where the restoring force of the actin cytoskeleton becomes equal to the drag force. The red line is the fit with the Kelvin-Voigt model $\varepsilon(t) = \frac{\sigma}{E}(1 - e^{-\lambda / t})$ and gives a σ/E value of 2.18 ± 0.02 µm and 7.38 ± 0.08 µm for (A) and (B), and a λ value of 0.29 ± 0.01 s^{-1} (A) and 1.2 ± 0.2 s^{-1} (B), respectively.

Bibliography

1. Casanova, D., D. Giaume, E. Beaurepaire, T. Gacoin, J.-P. Boilot, and A. Alexandrou. 2006. Optical in situ size determination of single lanthanide-ion doped oxide nanoparticles. *App. Phys. Lett.* 89:253103-1 – 253103-3.

2. Watanabe, N., T. J. Mitchison. 2002. Single-molecule speckle analysis of actin filament turnover in lamellipodia. *Science* 295:1083-6.